EUROPEAN ORGANIZATION FOR NUCLEAR RESEARCH

L3 Note # 2719
November 2, 2001

ISR Photons in W mass Analysis using the qqeν event sample

A. Gurtu[1,⋆] and M.A. Rahaman[2]

[1]CERN, Geneva and [2]Tata Institute of Fundamental Research, Mumbai

Abstract

Around 14% of $e^+e^- \to W^+W^-$ interactions at LEP are accompanied by the emission of initial state radiation with a photon of energy > 5 GeV. This leads to a reduction in the available center of mass energy and non-zero momentum of the e^+e^- system. Unless this is properly taken into account it leads to failure or distortion of the kinematic fits to the $e^+e^- \to W^+W^-$ reaction and consequently to a wrong determination of M_W. In this note we examine the issues using the L3 WW$\to$qqeν sample and report an improvement in the W mass resolution as well as the mean value of the fitted W mass.

⋆ On sabbatical leave from Tata Institute of Fundamental Research, Mumbai

1 Introduction

W mass determination at LEP is carried out by identification of $e^+e^- \to W^+W^-$events with at least one of the W's decaying hadronically, and then carrying out a kinematic fit to the events to obtain the fitted W mass(es). Plotting the probability distribution corresponding to the χ^2 of the fit, one observes that around 18-20% of the events have a fit probability, $P(\chi^2), < 5\%$. These are considered failed events and are not considered for eventual W mass extraction. Apart from bad measurement/reconstruction of events, one of the reasons for this large proportion of poor fits could be neglect of the ISR nature of (some of) the photons while clustering the event into 2 jets, and in the energy-momentum constraints applied in the kinematic fit. This is confirmed by the observation that the failed events ($P(\chi^2) < 5\%$) have an average photon energy, $<E_\gamma>$, $\simeq$ 6.5 GeV, compared to an $<E_\gamma>\simeq$ 3.3 GeV for the well fitted events ($P(\chi^2) > 5\%$). This is shown in figure 1 for L3 generator level energy distribution of photons in 189 GeV qqeν Monte Carlo. In the normalised ratio plot (fig. 2), it is seen that the so called failed events (with $P(\chi^2) < 5\%$) are more in the photon energy range between 5 to 25 GeV which is the typical initial state radiation (ISR) energy at $\sqrt{s}$ = 189 GeV. This strongly indicates that not taking proper care of ISR photon might be responsible for the failure of events in the kinematic fit. Moreover, if the ISR photon is not properly taken into account then it gets attached to one of the jets leading to a positive bias in the reconstruction of mass, even if the kinematic fit probability is $> 5\%$.

To take into account the effect of ISR in kinematic fits to the $e^+e^- \to W^+W^-$ reaction it is necessary to, firstly, identify a sufficiently high energy photon ($\sim$ 5 GeV or more) in the event, secondly, to classify it as an ISR photon, and, finally, to include it properly in the fit. If it is FSR then the present (L3 default) approach of clubbing it in the final state visible energy is, of course, perfectly valid. In L3, an early generator level study on ISR for the qqqq final state was made as far back as in 1993 [1] and more recently another study was made [2]. ALEPH have used detected photons successfully in their W mass analysis for the qqqq final state [3]. In this note we report our study on ISR photon in qqeν sample at energies 189 – 208 GeV.

2 Monte Carlo and Data

For this study the data collected in the years 1998, 1999 and 2000 is used. Table 1, shows the luminosity collected at center-of-mass energies. For Monte Carlo the signal events $e^+e^- \to W^+W^- \to ffff(\gamma)$ are generated by KORALW which takes into account ISR and FSR and main background events $e^+e^- \to q\bar{q}(\gamma)$ are generated by KK2F. The analysis is carried out in two steps. In the first, the default qqeν selection [4] and kinematic fitting is done; in the second step an ISR photon is searched for and, for those events where it is detected, it is treated as such, both in the selection as well as in the kinematic fit.

3 Selection of Photon

Monte Carlo (MC) studies show that most of the ISR photons are emitted parallel to the beam axis so it is necessary to select photons in low polar angle to increase the statistics. To select the photon in the low polar angle we use the luminosity monitor and active lead ring (ALR). A photon with high transverse momentum may also be detected in the central (barrel) and endcap regions which are covered by the BGO detectors.

The highest energetic cluster in the BGO with electromagnetic criteria and no associated TEC track is selected as a photon. The isolation of the selected photon is very important to know that is not part of any of the jets (FSR). The following cuts have been used to select a photon in the BGO barrel and endcap regions.

Energy	E_γ	$>$	5 GeV
EM Criteria	$E9/E25$	$>$	0.98
Isolation	$E_\gamma/E_{cone(15)}$	$>$	0.85
	$E^H_{cone(7)}/E_\gamma$	$<$	0.10
	$\alpha_{\gamma,obj}$	$>$	18°
No Charge	$\Delta\phi$	$>$	30 mrad (BARREL)
		$>$	60 mrad (ENDCAP)

Here $E9/E25$ is the ratio of energy deposit in the central 3 x 3 crystal array to that in the 5 x 5 crystal array; $E_{cone(15)}$ is the energy in a cone of half-angle 15 degrees around the photon direction; $E^H_{cone(7)}$ is the hadronic energy in a cone of half-angle 7 degrees around the photon direction; $\alpha_{\gamma,obj}$ is the angle between the photon and any object (track or jet) and $\Delta\phi$ is the azimuthal angle between the photon and the nearest charged track.

The sub-detector luminosity monitor and ALR cover the θ interval from 1.3° to 8.2°. As there is in no TEC behind this part of the detector, it is not possible to put a veto on the track in this region. Thus, in order to reduce background, the energy threshold for the photon is set higher, at $E_\gamma > 10$ GeV. Although this part of detector covers a very limited angular region, around 40% of the selected photons come from this sub-detector as ISR tends to follow the beam direction.

It is very important to avoid selecting final state radiation (FSR) photon. We have seen from MC studies that the ISR photon energy distribution dies off at about $\sqrt{s} - 2 \times M_W$ but for FSR photon it can go upto 70 GeV at $\sqrt{s} = 200$ GeV. Upper limit of ISR and FSR energy depends on center-of-mass energy. A photon is selected as an ISR photon if its energy lies in the interval,

$$
\begin{array}{rl}
5 \text{ GeV} < E_\gamma < \sqrt{s} - 2 \times M_W \text{ GeV} & \text{in barrel + endcap region} \\
10 \text{ GeV} < E_\gamma < \sqrt{s} - 2 \times M_W \text{ GeV} & \text{in lumi + ALR region}
\end{array}
$$

along with other cuts as specified above. About 20% of the emitted highest energetic photons come from FSR. After putting isolation and energy cuts we managed to bring it to about 10% in the selected photon sample.

4 The Kinematic Fit

For the kinematic fit we use the standard APWW package [5]. In usual case we use the matrix inversion method imposing the constraints of energy and momentum conservation and equal W masses (2C fit). The events with an identified photon in the detector are reclustered without photon (and electron) and the kinematic fit is perfomed with the modified constraints,

$$\left[\sum_{i=1}^{4}(E_i, \vec{P}_i) = (\sqrt{s}, \vec{0})\right] \quad \rightarrow$$

$$\left[\sum_{i=1}^{4}(E_i, \vec{P}_i) = (\sqrt{s} - E_\gamma, -\vec{P}_\gamma)\right]$$

We studied two kinds of fits: (i) Photon added to the χ^2 and (ii) fitting with only four particles (without photon) and we observe that the fit results are more or less same for both the cases which confirms very precise measurement of photon in the BGO. In this note, we have presented the results when photon is added to the χ^2 as a fifth particle.

5 Results

To study the effect of ISR photon in the kinematic fit, we carry out the kinematic fit of the qqeν events with an identified photon in the detector (we call this event as qqe$\nu\gamma$) considering the photon properly in the reconstruction and in the kinematic fit with modified constraints. The W mass resolution and fitted W mass distribution is fitted to a split function [6] consisting of a gaussian on one side and exponential on the other and quote the mean and sigma of the gaussian. This function is given by

$$f(x) = \begin{cases} A\ exp[-a(x - x_0)^2] & \text{if } x \geq x_c \\ B\ exp[b(x - x_0)] & \text{if } x < x_c \end{cases}$$

where $a = 1/(2\sigma^2)$, $b = -2a(x_c - x_0)$ and $B = A\ exp[-a(x - x_0)^2]$. There are four free parameters, three describing a gaussian (A, x_0, σ) and one (x_c) which splices in an exponential tail continuously. This function gives considerably better fits to resolutions with an asymmetric non-gaussian background superimposed upon a gaussian.

In table 2, we give the number of photons selected in MC and data at various center-of-mass energies. A look at column 6 confirms the point made in Sect 1 that the fitted W-mass gets a positive bias if an ISR photon is treated as part of a jet. As the average ISR photon energy increases with $\sqrt{s}$, one sees a clear increase in the bias from $\sim$ 4 GeV at 189 GeV to $\sim$ 7 GeV at 208 GeV.

5.1 Monte Carlo Studies

In what follows, figures will be presented only for 189 GeV center-of-mass energy. Results at other energies follow the same trends as at 189 GeV. This is evident from the means and widths of various distributions at all energies which are listed in table 2. One set of figures for 206 GeV data is given at the end of this sub-section to demonstrate this.

In fig. 3, we show the $P(\chi^2)$ of qqe$\nu\gamma$ events without considering photon in the clustering and kinematic fit. In fig. 4, we plot the $P(\chi^2)$ of the qqe$\nu\gamma$ events considering photon in the clustering and kinematic fit. One sees that in the second case the number of events in which the fit converges is less than in the first case. This is due to the extra contraint in the second fit due to the measured photon energy. But still the overall number of events with $P(\chi^2)\ > 5\%$

is greater in the second case, i.e., when we consider properly the photon in clustering and kinematic fit; this is shown in table 2 and is true for all energies.

In fig. 5, we show the W mass resolution. The left figure is for the fit when we do not consider photon as ISR and the right figure is for the fit when we consider the photon as ISR in the clustering of the event and in the kinematic fit. It is seen that both the mean and sigma is improved when the photon is taken into consideration as ISR during clustering and in kinematic fit. The mean of W-mass resolution is +4.2 GeV in the first case. This is because the photon gets attached to one of the jets leading to a positive bias in the mass determination. On the other hand, when the photon is considered as ISR in the kinematic fit the mean of the W-mass resolution is –0.5 GeV. (As we will show later this small negative bias is due to FSR photon contamination). In fig. 6, we show the fitted (2C) W-mass. Again in the left figure the photon is not considered as ISR and in the right figure it is. The mean as well as sigma of the fitted W-mass are improved by considering the photon as ISR as expected from the conclusions drawn from the previous figure 5.

Figures 5 and 6 demonstrated a small ($\sim$ 0.5 GeV) negative bias when we considered the photon as ISR in the fit, compared to a 3.5 GeV positive bias when we do not consider photon as ISR. To investigate this effect we match the photons selected in the detector to the generated ones and from generated photon information we tag the photons as ISR or FSR. Those detected photons which do not match any generated photon within specified energy and angular tolerances are ignored. From fig. 7 and fig. 8 one sees that the W-mass resolution and fitted W-mass have negligible bias if a photon has been correctly tagged as ISR but if an FSR photon is treated as ISR this leads to a large negative bias of 3.7 GeV. This explains the fact that when one consider all photons in the fit as due to ISR one gets a net 0.5 GeV negative bias because about 10% of the photons selected as ISR are in fact FSR photons.

About 40% of the selected qqe$\nu\gamma$ events have $P(\chi^2) < 0.05$ when the photon is not considered as ISR in the clustering of events and in the kinematic fit. The left side of fig. 9 shows the fitted W-mass of these events. One would like to confirm that when one takes the ISR effect properly into account a good proportion of these events should end up having their $P(\chi^2) > 0.05$ in the kinematic fit and also show an improvement in the mean value and sigma of the fitted mass distribution. The right side of fig. 9 shows the fitted W-mass when the photon is properly treated as an ISR and fig. 10 shows the $P(\chi^2)$ distribution of this kinematic fit. One sees from the plots that the fitted W-mass improves considerably from 87.2 GeV to 79.6 GeV whereas the resolution remains the same. One also notes that about half of the events now have $P(\chi^2) > 0.05$ and their $P(\chi^2)$ distribution goes upto $P(\chi^2) = 1$ and is flat except in the first few bins. This demonstrates that by properly taking into account the ISR nature of photons associated with "failed" events one can recover about half of them and improve significantly the fitted W-mass value.

All the above analysis for 189 GeV has also been carried out for each of other 6 energies between 192 to 208 GeV. In figs. 11 and 12 the fitted W-mass resolutions and fitted W-mass distributions are shown at 206 GeV. This completely confirms the conclusions drawn from 189 GeV data (figs. 5 and 6), regarding high positive bias of the fitted W-mass (87.2 GeV) and poorer sigma (7.0 GeV) when the ISR photon is not properly taken into account, compared to almost zero bias in the fitted W-mass (80.1 GeV) and better sigma (4.3 GeV) when ISR photons are properly handled. Similar behaviour is observed at all other energies also.

5.2 Data and Monte Carlo

All the data collected in the years 1998, 1999 and 2000 has been analysed. Out of a total of 1339 events selected as qqeν, the number of qqe$\nu\gamma$ events is 57 (29 in the BGO barrel/endcaps and 28 in the lumi monitor) compared to the Monte Carlo expectation of 48 events (28 and 20 respectively).

In fig. 13, we show the energy distribution of selected photons in the BGO and luminosity monitor plus active lead ring. In fig. 14, we show the θ distribution of selected photons. The data match well with the expectation from MC except for the small excess in the very low angular region.

In fig. 15, we show the fitted W-mass of all the data collected in the years 1998, 1999 and 2000 with an identified photon in the detector. In this case the photon has not been considered as ISR in clustering and kinematic fit. We see that the mean value of the fitted W-mass is 84.0 GeV which is an over-estimation by about 3.5 GeV if one compares with the world average value of 80.45 GeV. In fig. 16, we show the fitted W mass when the photon is considered as ISR in clustering and kinematic fit. The mean of fitted W mass is now quite reasonable and the sigma improves by about 25% for the events identified as qqe$\nu\gamma(ISR)$.

6 Discussion and Summary

We have seen from our studies that the average ISR photon energy increases with the increase in center-of-mass energy. So the effect of over-estimation of W mass also increases with $\sqrt{s}$ if the photon is not considered as ISR in the clustering and in the kinematic fit. This over-estimation is about 7 GeV at highest energy points ($\sqrt{s} = 206$ GeV). But the fitted W mass remains stable at about 80 GeV when we consider the photon as due to ISR, the slight negative bias being due to a small FSR photon contamination. We have demonstrated that one can recover about 50% of those failed events ($P(\chi^2) < 0.05$) which are accompanied by a tagged ISR photon which is subsequently properly taken into account in the clustering and kinematic fit. Our studies also show an improvement in the W mass resolution which eventually would give better overall estimation of the W mass.

Inspite of the above positive results of this study the overall improvement in the error on W-mass from qqeν events is estimated to be upto 2%. The reason for this small effect is the low probability of detection of photons that we classify as due to ISR. It is suggested that this same methodology be applied to qq$\mu\nu$ and qqqq events, the latter constituting a much larger sample. In the case of qqqq one could also carry out kinematic fits including an unseen ISR photon which escapes in the beam pipe. This cannot be done in qq$\ell\nu$ events because of an already missing neutrino. With such a systematic treatment of ISR photons in all channels one should be able to recover a significant fraction of events which fail in the kinematic fit ($P(\chi^2) < 0.05$) and also reduce the mass bias and improve the mass resolution.

Acknowledgement: We wish to thank Prof S.N. Ganguli for his keen interest and useful discussions.

References

[1] T. Aziz et al, W mass determination with the L3 detector [A first look], L3 Note 1474, 28 August 1993.

[2] S.N. Ganguli and N. Raja, Some observations of ISR effects on W events, L3 Note 2618, 25 October 2000.

[3] Measurement of the W mass and width in e^+e^- collisions at 189 GeV.
R. Barate *et al.* [ALEPH Collaboration], Eur. Phys. J.**C17** (2000) 241.

[4] Measurement of the W-Pair Production Cross Section and W-Decay Branching Fractions in e^+e^- Interactions at $\sqrt{s} = 189$ GeV
M. Acciarri *et al.* [L3 Collaboration], Phys.Lett.**B496**, 19 (2000)

[5] S. Banerjee et al, Introduction to the APWW Package, L3 Note 1947, 20 May 1996.

[6] C. Tully, "Baryon Production in Z Decay", Ph.D. thesis and L3 Note 2210, 1998, who quotes Philip E. Kaaret, "Forward Production of J/ψ in Hardronic Interactions and Calibration of a Large BGO EM Calorimeter", Ph.D. thesis, Princeton University, 1989.

Year	$\sqrt{s}$ (GeV)	$\mathcal{L}$ (pb^{-1})
1998	188.60	176.4
1999	191.60	29.7
	195.54	83.7
	199.54	82.8
	201.75	37.0
2000	205.08	78.6
	206.67	130.4
	208.15	8.7
Total		627.3

Table 1: The luminosity collected by L3 detector at different center-of-mass energies

$\sqrt{s}$ GeV	MC	No of Photon selected	Events with $P(\chi^2)$ $> 5\%$		Fitted M_W			
					Mean		sigma	
			Fit w/o photon	Fit with photon	Fit w/o photon	Fit with photon	Fit w/o photon	Fit with photon
188.60	wk029	1016	636	675	84.54	79.71	4.40	3.22
191.60	wk038	920	599	620	84.98	79.75	5.67	3.47
195.54	wk039	1995	1174	1381	85.63	79.44	6.11	3.77
199.54	wk040	1773	1000	1177	86.02	79.93	6.57	3.67
201.75	wk041	770	882	1129	86.14	80.16	6.16	3.63
205.08	wk060	1956	1052	1316	86.72	79.91	6.75	4.05
206.67	wk061	1712	903	1109	87.21	80.13	7.05	4.27
208.15	wk059	1053	521	692	87.47	80.19	7.84	3.56
All data collected in 1998, 1999 and 2000 together								
all data		57	31	35	84.31	79.69	5.73	5.43

Table 2: The table shows the number of events selected at various $\sqrt{s}$. There are improvements in mean and sigma of fitted W mass when we fit the events taking ISR nature of photons into account. The number of events with $P(\chi^2) > 0.05$ is also improved. The mean and sigma of the fitted W mass increases with $\sqrt{s}$ when we do not account properly for ISR photons in the kinematic fit; but when we do so, the mean of fitted W mass is close to the generated one and independent of $\sqrt{s}$. The sigma is also significantly lower and $\sqrt{s}$ independent.

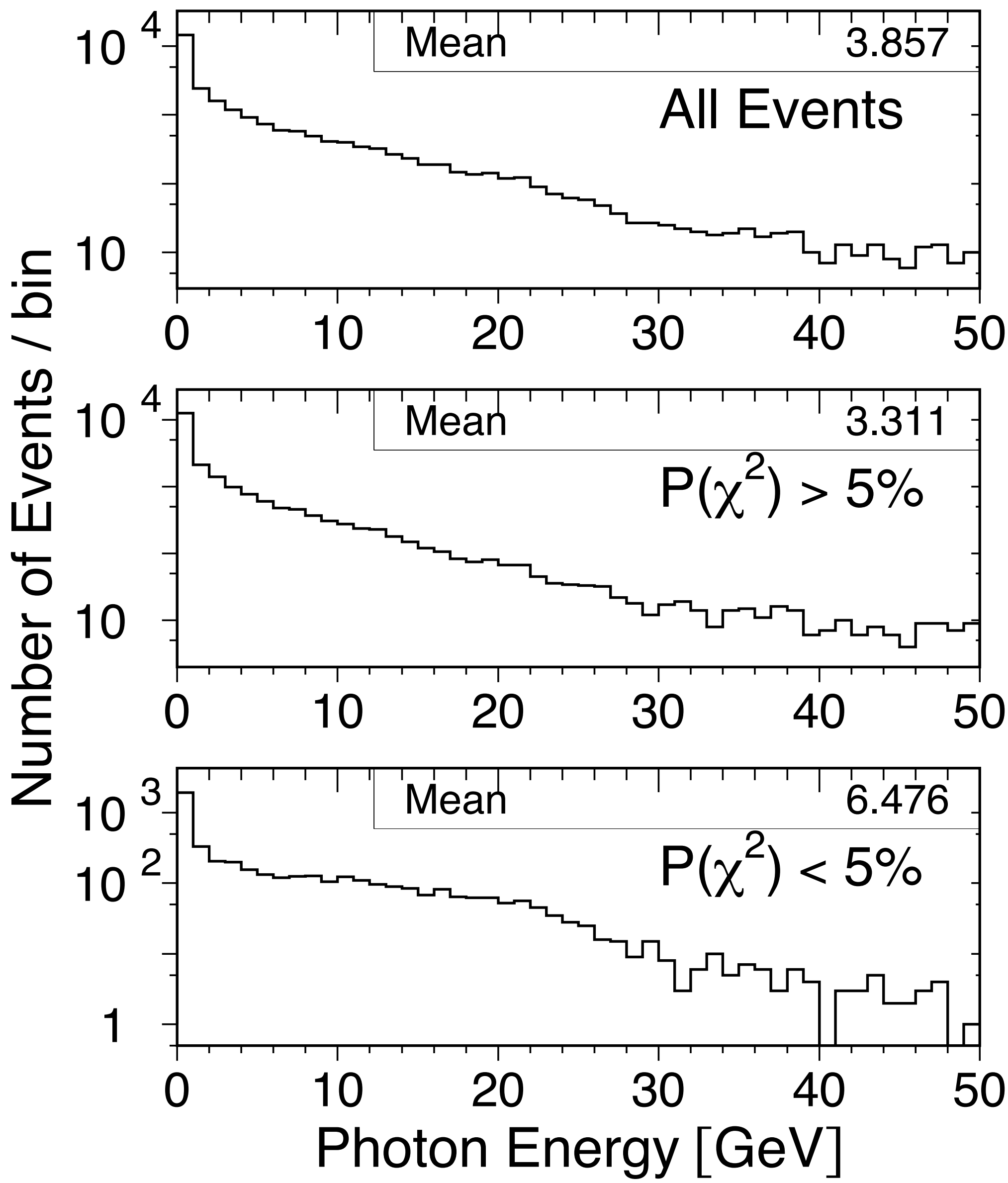

Figure 1: The distribution of generator level energy of the highest energy photon in qqeν sample at $\sqrt{s}$ = 189 GeV. Average photon energy for the events with $P(\chi^2) < 0.05$ is 6.5 GeV compared to the events with $P(\chi^2) > 0.05$ which have average photon energy 3.3 GeV.

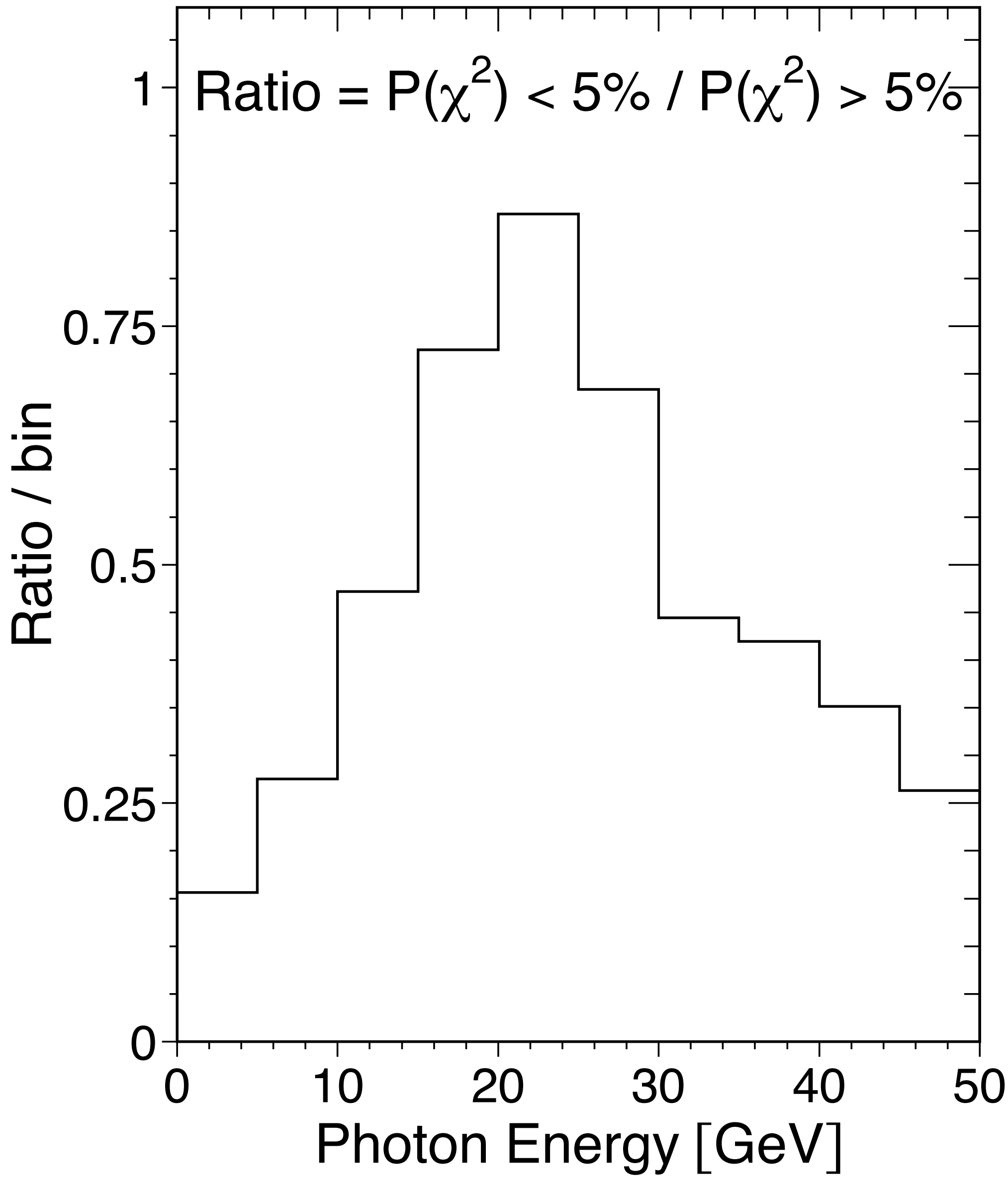

Figure 2: The plot shows that the number of events which have $P(\chi^2) < 0.05$ are more populated in the energy range 5 GeV to 25 GeV of the photon suggesting that failure to account for the ISR nature of the photon is responsible for failure in the kinematic fit.

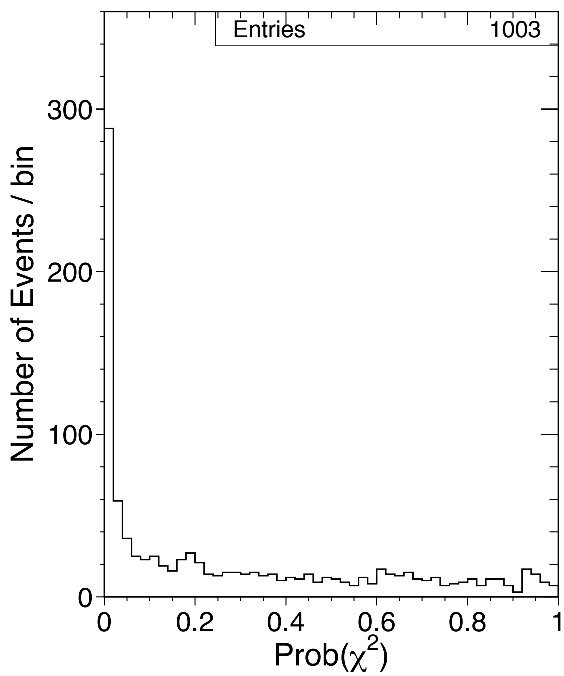

Figure 3: [**MC wk029** ($\sqrt{s}$ = 189 GeV)] The probability of χ^2 of events with an identified photon but without the photon being considered as ISR in the clustering and kinematic fit.

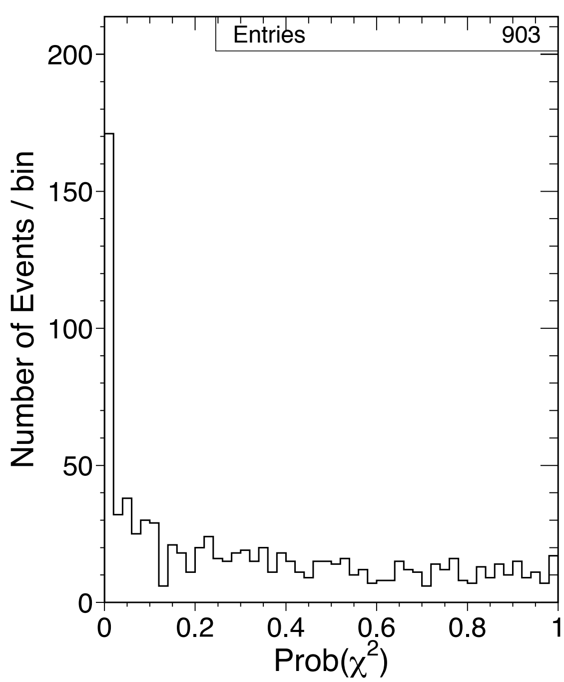

Figure 4: [**MC wk029** ($\sqrt{s}$ = 189 GeV)] The probability of χ^2 of events with an identified photon and the photon being considered as ISR in the reclustering and kinematic fit.

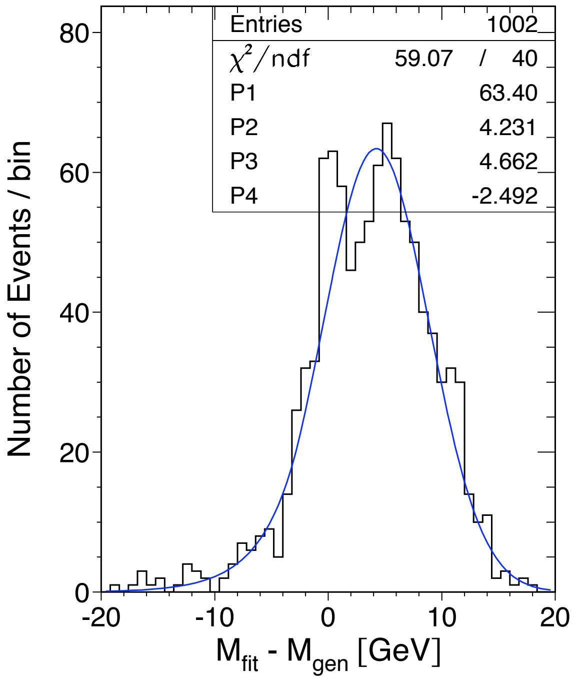

Figure 5: [**MC wk029** ($\sqrt{s}$ = 189 GeV)] The W mass resolution. Left fig when the photon was not considered as ISR and right fig when the photon was considered as ISR in the reclustering and kinematic fit

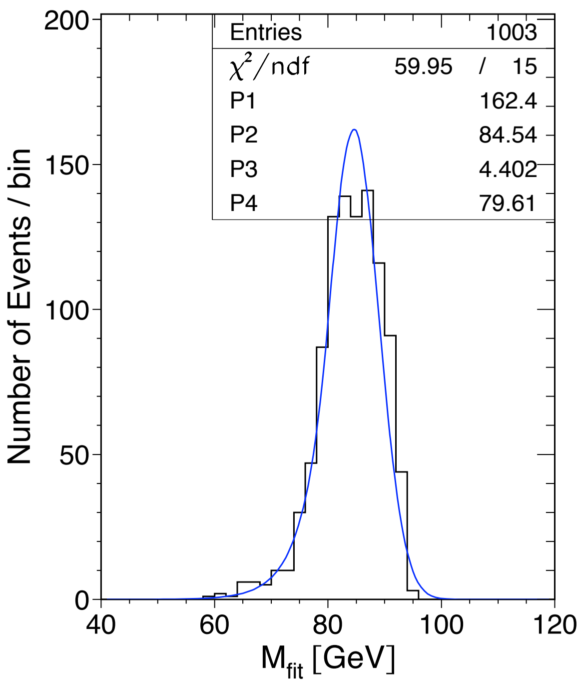

Figure 6: [**MC wk029** ($\sqrt{s}$ = 189 GeV)] The fitted W mass. Left fig when the photon was not considered as ISR and right fig when the photon was considered as ISR in the reclustering and kinematic fit

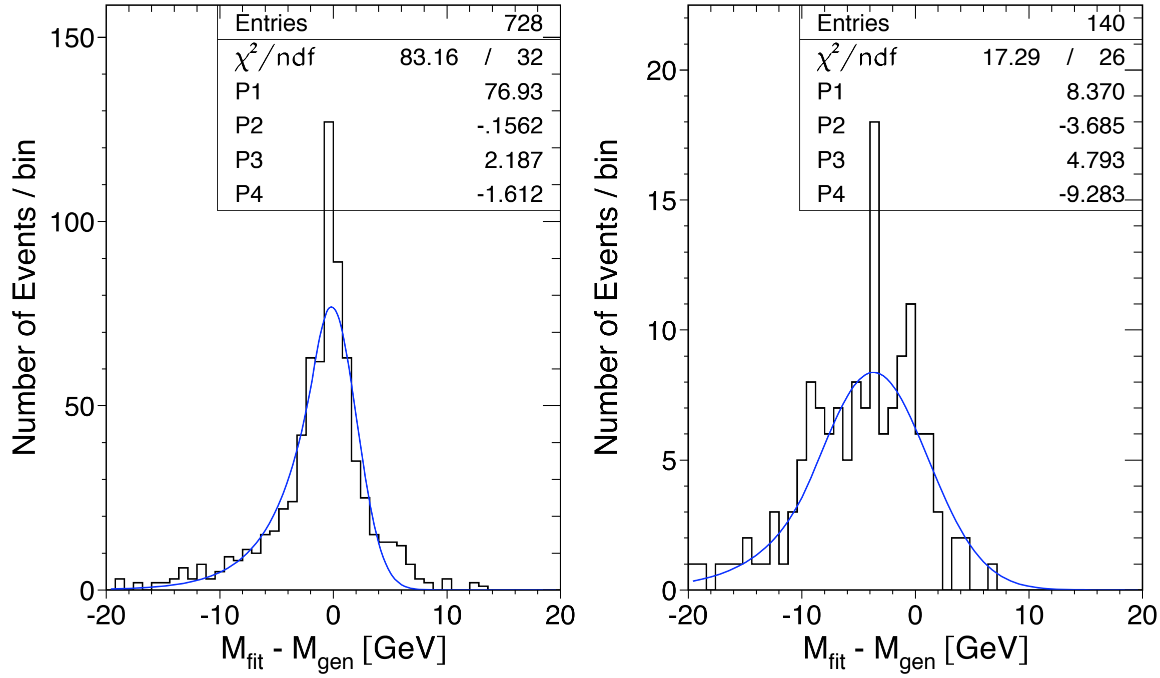

Figure 7: [**MC wk029** ($\sqrt{s}$ = 189 GeV)] The W mass resolution. Left fig for tagged ISR photon and right fig for tagged FSR photon. All photons considered as ISR in the reclustering and kinematic fit.

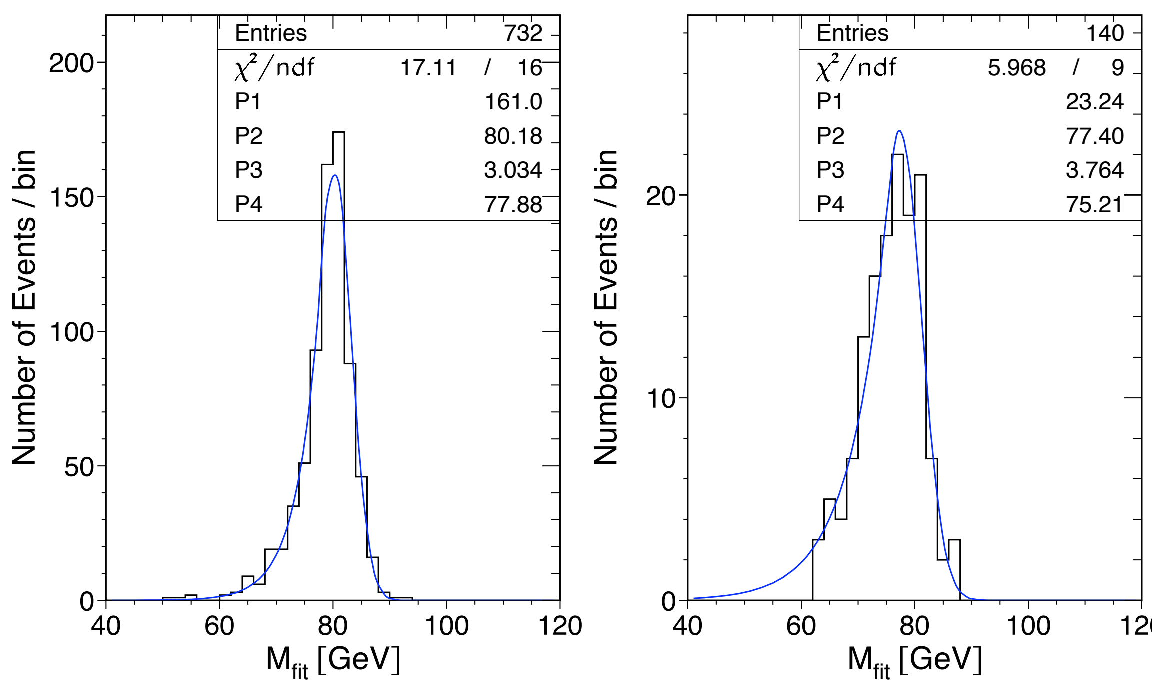

Figure 8: [**MC wk029** ($\sqrt{s}$ = 189 GeV)] The fitted W mass. Left fig for tagged ISR photon and right fig for tagged FSR photon. All photons considered as ISR in the reclustering and kinematic fit.

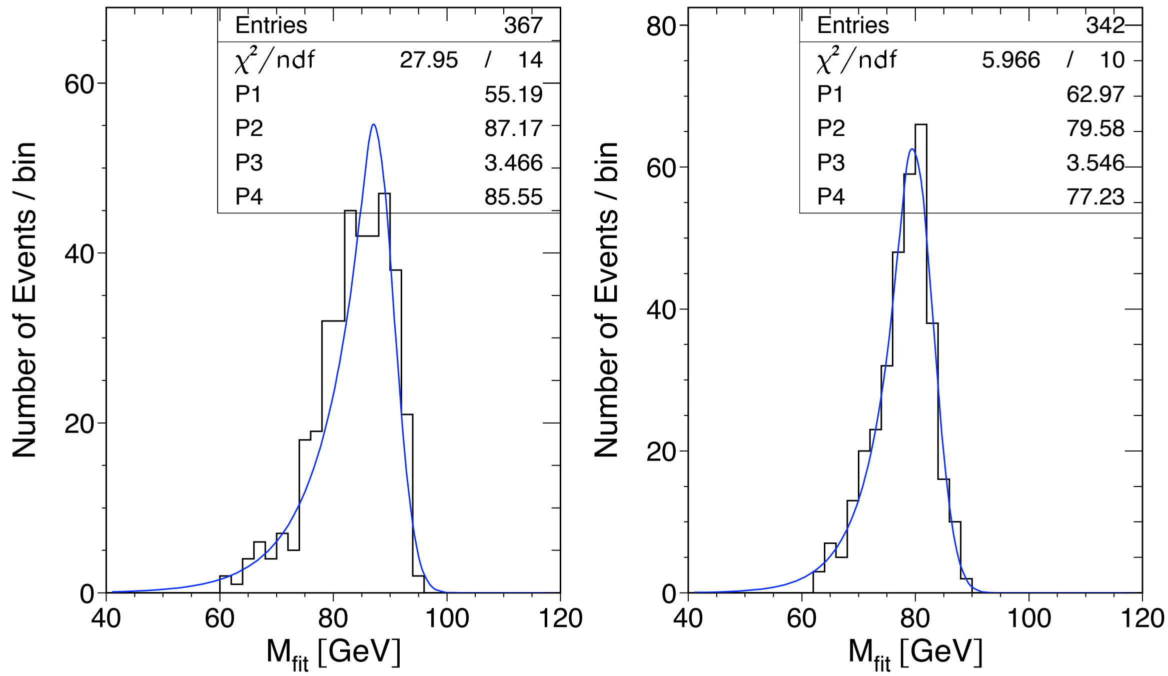

Figure 9: [**MC wk029** ($\sqrt{s}$ = 189 GeV)] The fitted W mass of the subset of events which have $P(\chi^2) < 0.05$ when fitted without considering the photon as ISR. Left fig when the photon was not considered as ISR and right fig when the photon was considered as ISR in the reclustering and kinematic fit.

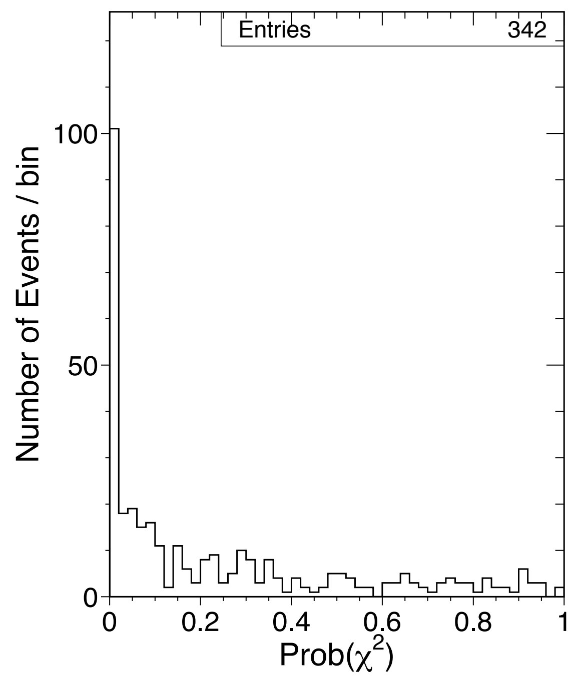

Figure 10: [**MC wk029** ($\sqrt{s}$ = 189 GeV)] The probability of χ^2 distribution of refitted events which had $P(\chi^2) < 0.05$ when first fitted without considering the photon as ISR. It is seen that half of the events now have $P(\chi^2) > 0.05$ when the photon is considered as ISR. The distribution is flat and extends to 1.

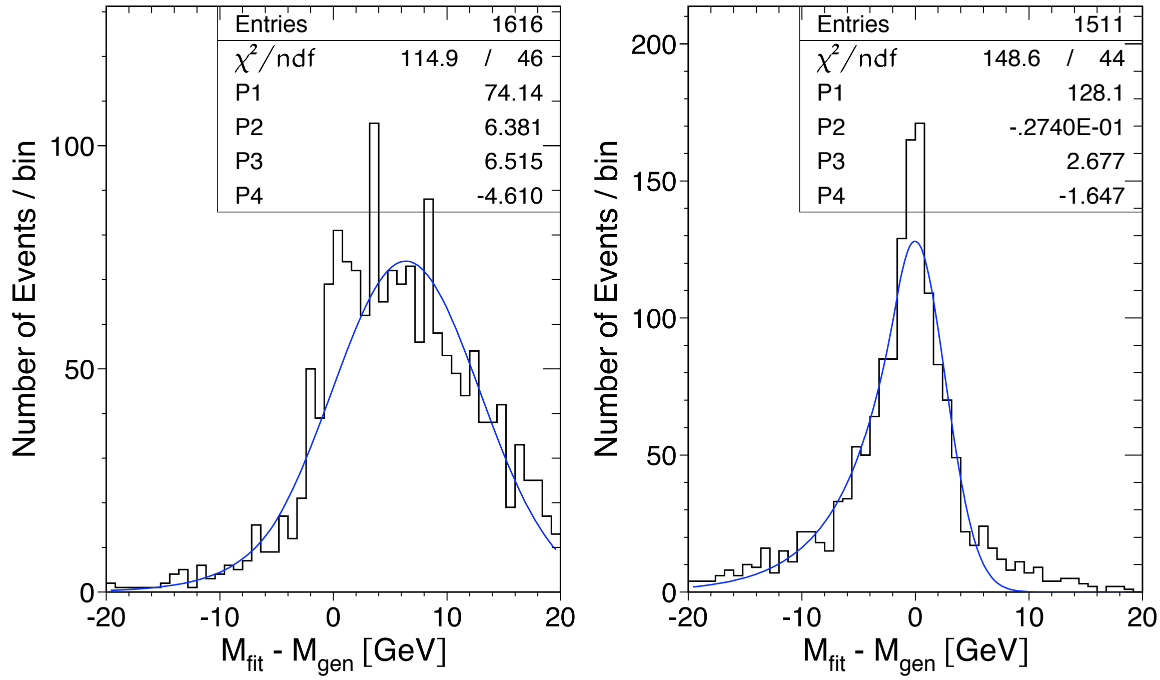

Figure 11: [**MC wk061** ($\sqrt{s}$ = 206 GeV)] The W mass resolution. Left fig when the photon was not considered as ISR and right fig when the photon was considered as ISR in the reclustering and kinematic fit

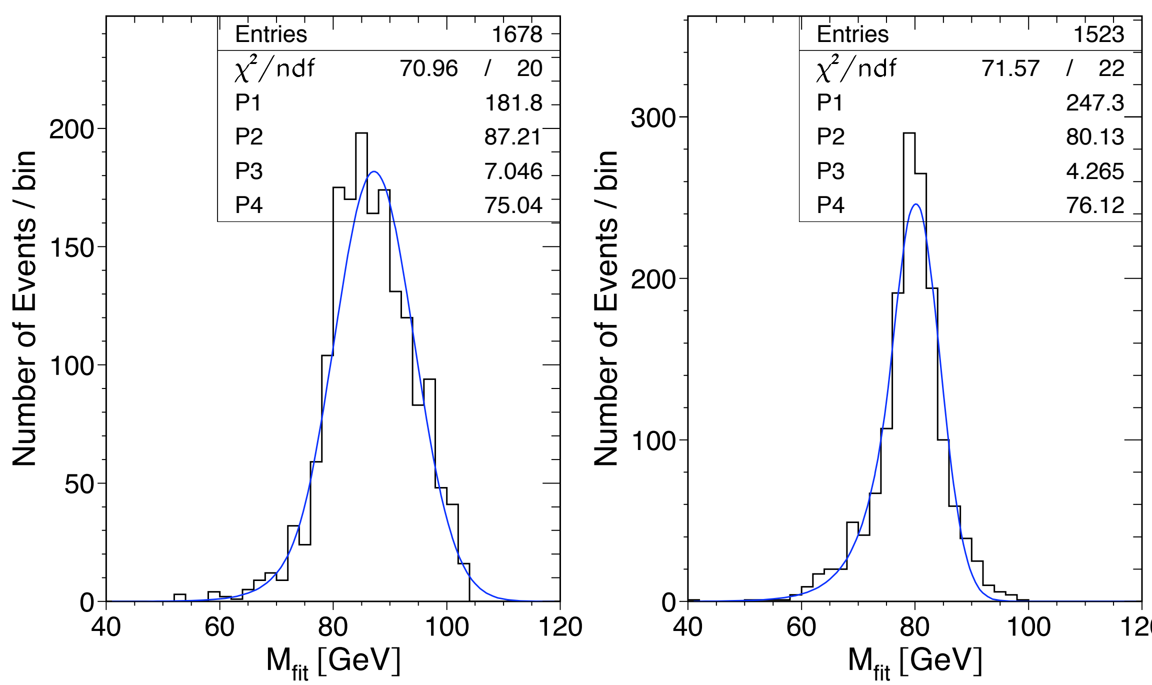

Figure 12: [**MC wk061** ($\sqrt{s}$ = 206 GeV)] The fitted W mass. Left fig when the photon was not considered as ISR and right fig when the photon was considered as ISR in the reclustering and kinematic fit

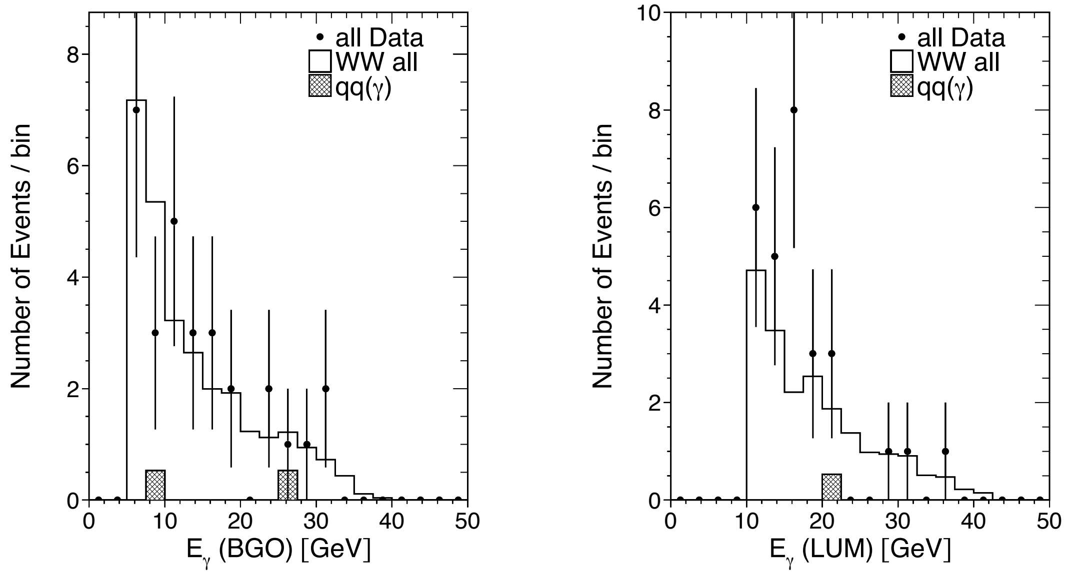

Figure 13: [**Data (1998,1999,2000)**] The energy distribution of selected photons. Data added together for all years.

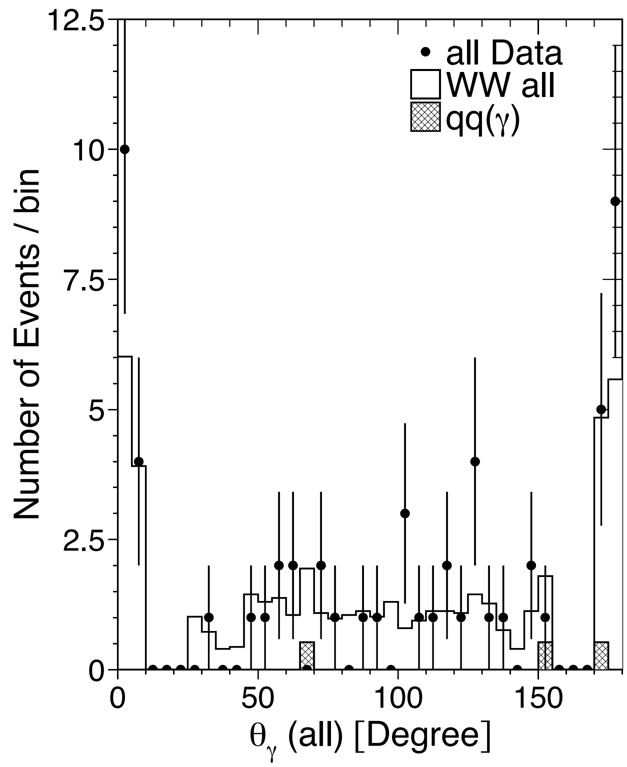

Figure 14: [**Data (1998,1999,2000)**] Theta distribution of selected photons. Data added together for all years.

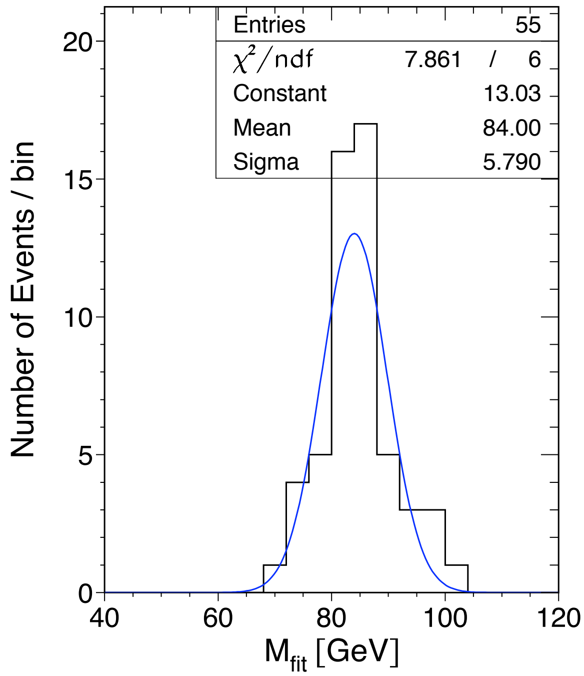

Figure 15: [**Data (1998,1999,2000)**] The fitted W mass of all data with an identified photon. But the photon has not been considered as ISR in the clustering of events and kinematic fit

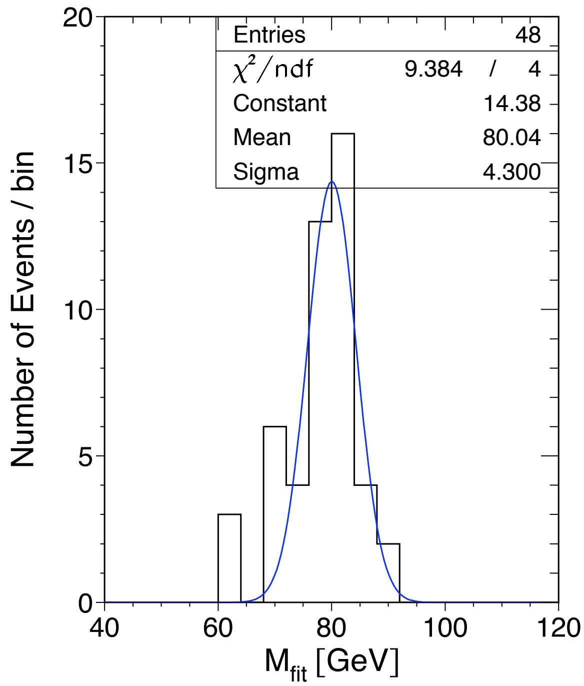

Figure 16: [**Data (1998,1999,2000)**] The fitted W mass of all data with an identified photon. The photon has been considered as ISR in the event clustering and kinematic fit